



Performance evaluation of a reinforced concrete building strengthened respectively by the infill wall, active and passive tuned mass damper under seismic load

Osman Akyürek^a, Nakin Suksawang^{b,*}, Tiauw Hiong Go^c, Hamide Tekeli^d

^a Department of Civil Engineering, Nevsehir Haci Bektasi Veli University, Nevsehir, Turkey

^b Department of Mechanical and Civil Engineering, Florida Institute of Technology, 150 W University Blvd, Melbourne, FL 32901, United States

^c Department of Aerospace, Physics and Space Science, Florida Institute of Technology, 150 W University Blvd, Melbourne, FL 32901, United States

^d Department of Civil Engineering, Suleyman Demirel University, Isparta, Turkey

ARTICLE INFO

Article history:

Received 1 November 2018

Accepted 8 July 2019

Available online 2 August 2019

Keywords:

Tuned mass damper (TMD)

Active tuned mass damper (ATMD)

Linear quadratic regulator (LQR)

Masonry infill wall

Reinforced concrete (RC) building

ABSTRACT

One of the most commonly used control methods is a tuned mass damper (TMD), which is often employed to mitigate the amplitude of mechanical vibrations. To get a more effective response reduction of the structure, it is essential that the dynamics of the structure are modeled as accurately as possible. In this study, the seismic response of a reinforced concrete (RC) six-story building was analyzed with the combinations of masonry infill-wall, a passive and an active tuned mass damper (ATMD). The infill walls were placed along all frames without any space between column-wall and beam-wall connection. The TMD has no external source of energy, while the ATMD has an external energy source generated by the actuator which is driven by a linear quadratic regulator (LQR) controller. The dynamic response of the building was evaluated using the data from a real earthquake excitation of El Centro in 1940. The results highlight the inclusion of masonry infill wall in the seismic analysis is very important and has a substantial effect on the fundamental frequency and seismic characteristic of the structure. It also has a significant impact on the reduction of the inter-story drift and the seismic energy performance of the building.

© 2019 Elsevier Ltd. All rights reserved.

1. Introduction

In the last two decades, there has been significant attention to the development of control systems to dissipate the earthquake ground motion on buildings. The control systems can be divided into passive, active [1,2], semi-active [3] and hybrid control strategies [4] proposed to enhance the safety and performance of structures induced by various dynamic loadings such as an earthquake.

Passive control systems are external supplemental devices on a structure to dissipate exposed dynamic energy and suppress the response of the structure under dynamic loads without external power sources. These systems are widely used and easy to implement on buildings because of their effectiveness in mitigating severe dynamic load effects. They are simple to understand, reliable and do not have the potential to destabilize the buildings.

The infill wall can be categorized as a passive control system since it acts as a passive energy dissipater (PED). In many reinforced concrete (RC) buildings, the infill wall is mostly ignored in structural analysis and widely used for architectural design purpose, however, it does also have a significant effect on seismic analysis, particularly its impact on the period, the lateral load capacity, and the total dissipated energy of the building [5–10]. Furthermore, the influence of infill wall placement on the dynamic behavior of various passive control strategies such as tuned mass damper (TMD) [11] and tuned liquid dampers (TLDs) [12] in the RC buildings under seismic excitation have currently been paid attention.

Another most commonly and intensively used passive control strategy, thanks to its simplicity and costs, is a tuned mass damper (TMD). It adds an external damping, stiffness, and mass to the main structure without using any external energy sources to resistant to strong ground motions or severe wind gusts [13–15]. However, TMD might not be the most comprehensive way to enhance the safety of the structure because of some drawbacks. The effectiveness of TMD is significantly affected by mistuning, which can

* Corresponding author.

E-mail addresses: nsuksawang@fit.edu (N. Suksawang), tgo@fit.edu (T.H. Go), hamidetekeli@sdu.edu.tr (H. Tekeli).

increase undesirable vibration on a structure. It can be solely tuned to the fundamental frequency of the structure so that it is only effective in the small range of frequency. It may have little or no effect for other modes that are not used for its tuning process in the scenario of a dynamic load.

In overcoming such problems of TMDs, an active control strategy (ATMD) has been widely proposed using the same TMDs equipment but with the inclusion of external energy sources provided by an actuator. However, putting vast amounts of external actuator energy on the system is not always possible. Even when it is possible, it can destabilize the structure in contrast to a passive controller. Therefore, it needs to be optimized for the desired design perspective and the optimum force needs to be driven by control methods such as proportional-integral-derivative (PID) [16], linear quadratic regulator (LQR) [17], and linear quadratic gaussian (LQG) [18]. All these control methodologies have been successfully applied to civil structures to generate the optimal force from the actuators under severe dynamic loading by many engineers and researchers [19–21].

This study focuses on the performance of masonry infill wall, which is generally neglected in the design, in a 6-story RC building under seismic load. Additionally, the performance of the masonry infill wall was compared to other seismic control strategies including the use of TMD and ATMD. The infill walls were placed along all frames without any space between column-wall and beam-wall connection. For an active control system, the control force is generated by the actuator of ATMD, which is driven by LQR. The LQR using a genetic algorithm for an optimization of the weighting matrix [17,22–24] was employed. Matlab&Simulink [25] was used to simulate the system under real-time excitation data of the El Centro earthquake in 1940.

2. Description of model buildings to determine the effective placement of the infill wall

Phase 1 of the study was used to determine the impact of the infill wall placement in different plans of the structure. The seismic performance evaluation was performed with different infill wall placement layouts in the plan on the designed models by varying number of span and story. Model 1 is a bare 5-story 3×3 -bays RC building without the infill wall, while Model 2 is fully placed by infill wall. Model 3 has only exterior infill wall placement layouts and Model 4 has only interior axes placed with the infill wall. Model 5 is placed by the infill wall in an asymmetrical way, see Fig. 1.

The seismic performances of RC model buildings with and without infill wall were determined by using pushover nonlinear static analysis of structural analysis program (SAP 2000, 2011). The effects of the rate (area of infill wall to floor plan) and the placement layouts (symmetrical or asymmetrical) of infill wall were investigated in the model buildings to examine inter-story drift, torsional irregularity coefficient, capacity curve, fundamental period, sway demand in the roof story, damage level of columns in the base floor, building performance level. Damage levels were catego-

rized into four: operational (OP), immediate occupancy (IO), life safety (LF), and collapse prevention (CP). In order to show the effectiveness of infill wall placement layouts especially when it is symmetrically placed, the obtained results showed that symmetrically fully placed infill wall contributed to RC performance positively, see Table 1, whereas asymmetrical placement of infill wall in the building may lead the building to increase damage levels in the structural elements, see Table 2. For more details, readers are referred to [6]. To this end, Model 2 was adopted and evaluated further to compare with other control strategies.

3. Model overview and theory of the equivalent compression strut

3.1. Overview of RC building with control systems and applied seismic load

In Phase 2 of the study, a 6-story RC building is modeled with the same plane view of model buildings as Phase 1. The building is subjected to the N-S component of earthquake load happened in El Centro (1940), see Fig. 2. Fig. 3 illustrate the symmetrical building that gives the same response from N-S and E-W directions. In order to analyze the contribution of the infill wall on structural control, the seismic response of the RC shear-building is analyzed with the combinations of masonry infill-wall, a passive, and an active tuned mass damper. The infill walls are placed fully (like model 2) and symmetrically along all frames without any space between column-wall and beam-wall connection.

The RC building elevation is illustrated in Fig. 4a. When it is strengthened by masonry infill wall placement, it is shown in Fig. 4b. The implementations of TMD and ATMD are respectively illustrated in Fig. 4c and d. The simplified equivalent system used in the seismic analysis is illustrated in Fig. 4e.

3.2. Theory of the equivalent compression strut

The stiffness contribution of the infill wall is considered by modeling it as equivalent compression strut. It is assumed that it only works under compression in-plan direction and cannot handle any loads under tension. Additionally, it is also assumed that the infill wall does not have deformation capacity when it is laterally loaded out-of-plan. All analyses are performed in the elastic range.

In Fig. 5, θ is the angle between the height and length of the masonry wall and the thickness of the wall (t_{wall}) is 120 mm. H_{wall} , H_k and L_{wall} , L_k are respectively the height and length of the equivalent compression strut and frame. The diagonal length of the equivalent compression strut is defined as r_{wall} , the width of the strut is a_{wall} [26], which is given as:

$$a_{wall} = 0.175(\lambda_{wall} H_k)^{-0.4} * \Gamma_{wall} \quad (1)$$

where,

$$\lambda_{wall} = \left[\frac{E_{wall} t_{wall} \sin(2\theta)}{4E_c I_c H_{wall}} \right]^{\frac{1}{4}} \quad (2)$$

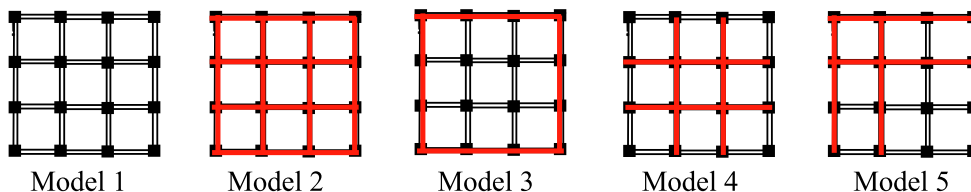


Fig. 1. The infill wall placement in the plan for 5-story 3×3 -bays; red color represents fully infill wall placement into the frame.

Table 1
Inter-story drift ration of the 3 × 3-bay 5-story model building, taken it from [6].

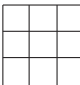
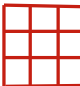
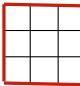
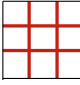
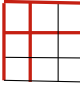
Type of model	Story no	Displacement at the ith floor di (m)	Relative displacement Δ _i (m)	δ _i = Δ _i × R (m)	Story height hi(m)	Inter-story drift ratio (δ _i) _{max} /h _i
Model 1 	0	0.000	–	0.000	–	0.000
	1	0.002	0.002	0.020	3	0.001
	2	0.006	0.003	0.024	3	0.001
	3	0.008	0.003	0.021	3	0.001
	4	0.010	0.002	0.015	3	0.001
	5	0.011	0.001	0.008	3	0.000
Model 2 	0	0.000	–	0.000	–	0.000
	1	0.002	0.002	0.013	3	0.001
	2	0.004	0.002	0.015	3	0.001
	3	0.005	0.002	0.013	3	0.001
	4	0.006	0.001	0.009	3	0.000
	5	0.007	0.001	0.005	3	0.000
Model 3 	0	0.000	–	0.000	–	0.000
	1	0.002	0.002	0.016	3	0.001
	2	0.004	0.002	0.019	3	0.001
	3	0.006	0.002	0.016	3	0.001
	4	0.008	0.001	0.011	3	0.000
	5	0.009	0.001	0.006	3	0.000
Model 4 	0	0.000	–	0.000	–	0.000
	1	0.002	0.002	0.016	3	0.001
	2	0.004	0.002	0.019	3	0.001
	3	0.006	0.002	0.016	3	0.001
	4	0.008	0.001	0.011	3	0.000
	5	0.008	0.001	0.006	3	0.000
Model 5 	0	0.000	–	0.000	–	0.000
	1	0.002	0.002	0.014	3	0.001
	2	0.004	0.002	0.017	3	0.001
	3	0.006	0.002	0.014	3	0.001
	4	0.007	0.001	0.010	3	0.000
	5	0.008	0.001	0.005	3	0.000

Table 2
Damage level at the first story columns for 3 × 3-bay 5-story model building, taken it from [6].

Damage level	Model 1		Model 2		Model 3		Model 4		Model 5	
	Number	Per. (%)	Number	Per. (%)	Number	Per. (%)	Number	Per. (%)	Number	Per. (%)
OP	4	25	8	50	3	19	6	38	4	25
IO	12	75	8	50	13	81	10	63	9	56
LS	0	0	0	0	0	0	0	0	2	13
CP	0	0	0	0	0	0	0	0	1	6
Total	16	100	16	100	16	100	16	100	16	100

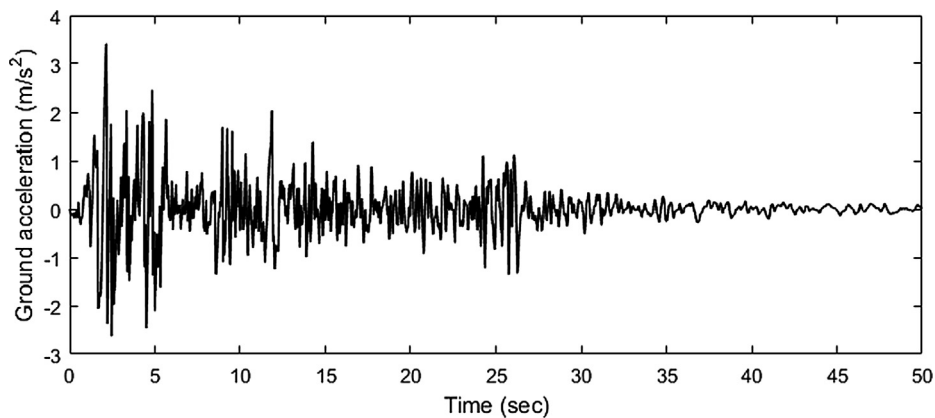


Fig. 2. El Centro (North-South) ground acceleration, in 1940.

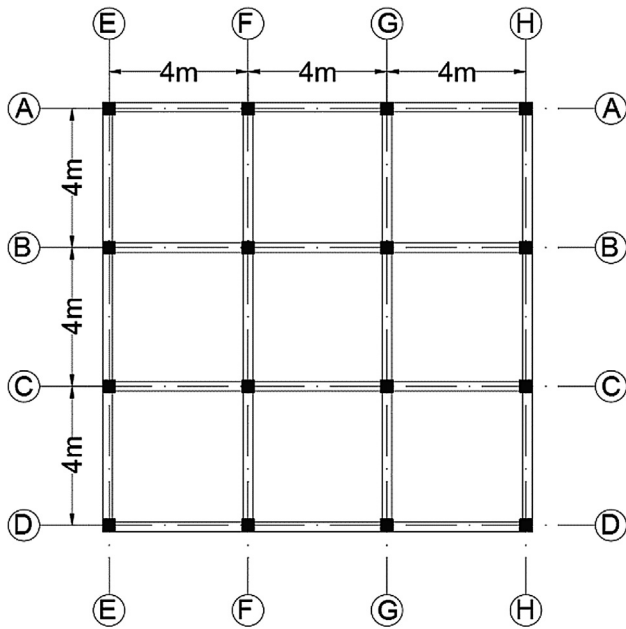


Fig. 3. RC building in plan-view.

The masonry wall is made of clay bricks with the modular size of 102 mm × 203 mm × 68 mm. The material properties of the infill wall are taken from the experimental study conducted by [5] and properties of structural components are provided in Table 3.

Assuming that the slab for each floor behaves as a rigid diaphragm, the response for each node of the floor is relative to one another under an earthquake force. Considering that flexural rigidity of the beams is infinite, the lateral stiffness of columns and the stiffness contribution of the infill wall are respectively calculated by using Eqs. (3) [27] and (4) [28] shown below. The damping contribution of the infill wall is taken from the experimental work [5] by a 33% increase in the damping ratio as compared to the bare RC building. The weight of the lateral load resisting members, columns, and beams, as well as infill walls, are neglected in time history analysis.

$$k_{col} = \frac{12E_c I_c}{H_k^3} \tag{3}$$

$$k_{wall} = \frac{G_{wall} L_{wall} t_{wall}}{H_{wall}} \tag{4}$$

where G_{wall} is the shear modulus of the infill wall and the other terms are as previously defined.

The Rayleigh method is employed in order to compute damping, which is viscous damping that is proportional to a linear

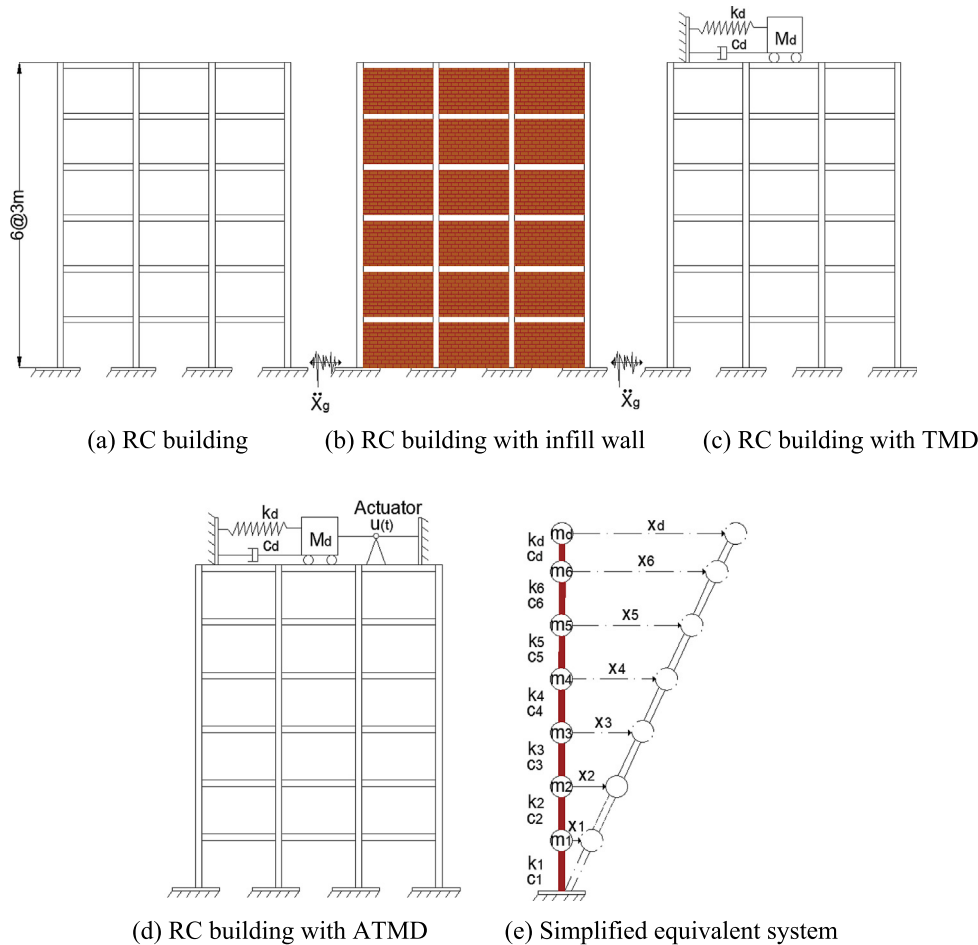


Fig. 4. Elevation-views of models in A-A direction with or without either TMD or ATMD whether including masonry infill walls or not.

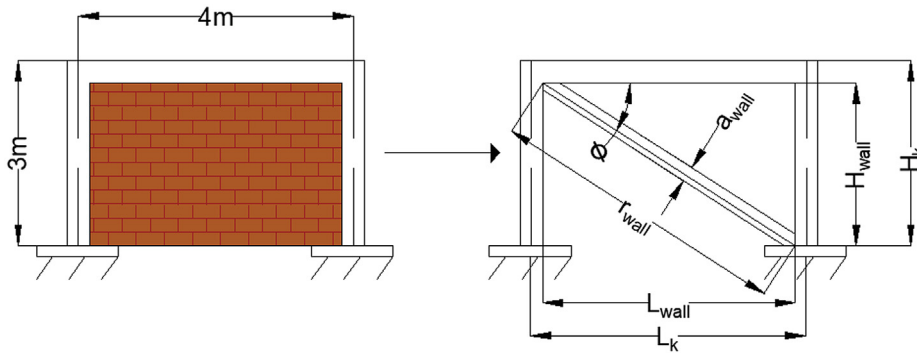


Fig. 5. The equivalent diagonal strut for infill wall representation (FEMA strut model) [26].

Table 3
Material and element properties of the structure.

Type of components	Size (mm)	Compression strength (MPa)	Modulus of elasticity (GPa)	Poisson's ratio	Density (kg/m ³)
Beams	300 × 500	20	28	0.15	2400
Columns (fc, Ec)	350 × 350	20	28		2400
Slabs	150	20	28		2400
Masonry wall (fwall, Ewall)	2500 × 3650	17	6.19		1500

combination of mass and stiffness. The damping ratio for the *n*th mode of such a system is

$$\begin{Bmatrix} \xi_i \\ \xi_j \end{Bmatrix} = \frac{1}{2} \begin{bmatrix} \frac{1}{\omega_i} & \omega_j \\ \frac{1}{\omega_j} & \omega_i \end{bmatrix} \begin{Bmatrix} a_0 \\ a_1 \end{Bmatrix} \quad (5)$$

In which, ω_i and ω_j are respectively *i*th and *j*th natural frequencies of the system, so the proportionality constants can be obtained as;

$$a_0 = \xi \frac{2\omega_i\omega_j}{\omega_i + \omega_j}, \quad a_1 = \xi \frac{2}{\omega_i + \omega_j} \quad (6)$$

where a_0 and a_1 are constants of proportionality and ξ is the damping factor or damping ratio. The damping factor for a model building is taken 4.30% and for the models with the infill wall is 5.7% by 33 percent increase to the model without infill wall placement [5]. The damping matrix C is governed as:

$$C = a_0M + a_1K \quad (7)$$

Table 4 summarizes the dynamic properties, including mass, damping, and stiffness, used in various building models.

4. Structural dynamics and control theory

4.1. Mathematical modeling for the RC shear building

Assuming that 6 story RC building has a six-degree-of-freedom and subjected to a one-dimensional base excitation in A-A direction. The equation of motion can be expressed as;

$$MX''(t) + CX'(t) + KX(t) = HU(t) + MEX''_g(t) \quad (8)$$

Table 4
The dynamic properties of the structure and TMDs.

Type of models	Dynamic properties for each floor		
	Mass (tonne)	Damping (kN s/mm)	Stiffness (kN/mm)
RC building	51.84	0.324	249
Infill wall	1.64	0.493	472
Contribution			
TMD properties	15.55	0.687	3.85

$$M = diagonal[m_1, m_2, m_3 \dots m_n]$$

$$C = \begin{bmatrix} c_1 + c_2 & -c_2 & & & & & \\ -c_2 & c_2 + c_3 & -c_3 & & & & \\ & -c_3 & \dots & & & & \\ & & \dots & \dots & & & \\ & & & \dots & c_n & & \\ & & & & c_n & c_n + c_d & -c_d \\ & & & & & -c_d & c_d \end{bmatrix}$$

$$K = \begin{bmatrix} k_1 + k_2 & -k_2 & & & & & \\ -k_2 & k_2 + k_3 & -k_3 & & & & \\ & -k_3 & \dots & & & & \\ & & \dots & \dots & & & \\ & & & \dots & k_n & & \\ & & & & k_n & k_n + k_d & -k_d \\ & & & & & -k_d & k_d \end{bmatrix}$$

where M, C, and K are respectively the *n* × *n* matrix of mass, damping, and stiffness of the structure including a tuned mass damper (TMD). Prime (′) represents derivative respect to time. X(*t*) is the *n*-dimensional displacement vector to the base excitation, U(*t*) is the control force vector, and H is the location vector of the controllers. E is the modification vector of the earthquake excitation. Then state space representation of Eq. (8) can be written as;

$$Z'(t) = AZ(t) + BU(t) + Wx''_g(t) \quad (9)$$

$$X(t) = C_r Z(t) + D_r U(t) \quad (10)$$

$$Z(t) = \begin{bmatrix} X(t) \\ X'(t) \end{bmatrix} \quad A = \begin{bmatrix} zeros(n, n) & eye(n, n) \\ -M^{-1}K & -M^{-1}C \end{bmatrix}$$

$$B = \begin{bmatrix} zeros(n, m) \\ M^{-1}H \end{bmatrix} \quad W = \begin{bmatrix} zeros(n, 1) \\ E \end{bmatrix}$$

$$C_r = [eye(n, n) \quad zeros(n, n)] \quad D_r = [zeros(n, 1)]$$

where Z(*t*) is the (2*n* × 1) state vector, A is the (2*n* × 2*n*) system matrix, B is the (2*n* × *m*) input matrix. W is an appropriate

$(2n \times 1)$ vector. C_r ($n \times 2n$) and D_r ($n \times 1$) are the output matrix and direct transmission matrix respectively. They are defined according to the desired output. In this condition, the desired output of state space is displacement.

4.2. Energy equation of the system

The general equation of motion for an MDOF system can be expressed in terms of energy computation as [29]:

$$\int_0^t \dot{X}'^T(\tau)MX''(\tau)d\tau + \int_0^t \dot{X}'^T(\tau)CX'(\tau)d\tau + \int_0^t \dot{X}'^T(\tau)KX(\tau)d\tau \\ = - \int_0^t \dot{X}'^T(\tau)MEX''g(\tau)d\tau + \int_0^t \dot{X}'^T(\tau)HU(\tau)d\tau \quad (11)$$

The energy equations can be written as [23]:

$$E_{kr} + E_d + E_a = E_{ir} + E_{ac} \quad (12)$$

In which E_{tir} is total input energy, which is equal to the sum of E_{ir} and E_{ac} , E_{kr} is relative kinetic energy, E_d is the damping energy, E_a is the strain energy and E_{ir} stands for the relative input energy, E_{ac} is the actuator energy, as formulated below:

$$E_{kr} = \frac{1}{2} \dot{X}'^T(t)MX'(t)$$

$$E_d = \int_0^t \dot{X}'^T(\tau)CX'(\tau)d\tau$$

$$E_a = \int_0^t \dot{X}'^T(\tau)KX(\tau)d\tau$$

$$E_{ir} = - \int_0^t \dot{X}'^T(\tau)MEX''g(\tau)d\tau$$

$$E_{ac} = \int_0^t \dot{X}'^T(\tau)HU(\tau)d\tau$$

4.3. Optimum fundamental properties of the tuned mass damper (TMD)

There are two definitions for tuning process called optimum (tuning TMD to the exact first frequency) and sub-optimum design (tuning it to a lesser frequency). In this study, sub-optimal design is taken into consideration of a TMD system because, according to Chey, Chase, et al. [30], the sub-optimum TMD system exhibits better response reductions than the corresponding optimum TMD system in terms of displacement, while the optimum TMD building system provides better acceleration reductions due to having higher damping ratios.

In the tuning process, the first thing is done by selecting the effective mass ratio of the structure and TMD as $\mu = \frac{m_d}{m} = 5\%$, where m_d is the mass of TMD. The damping ratio (ξ_d) and natural frequency (ω_d) of the TMD are obtained by using modified Den Hartog equations [31]:

$$\xi_d = \sqrt{\frac{3\mu}{8(1+\mu)} + \frac{0.1616\xi}{1+\mu}} \quad (13)$$

$$\omega_d = q\omega_n \quad (14)$$

In which, q is the frequency ratio of the TMD and the structure, obtained as:

$$q = \frac{1}{1+\mu} (1 - 1.5906\xi) \sqrt{\frac{\mu}{1+\mu}} \quad (15)$$

The damping (ξ_d) and frequency (q) ratios are computed using Eqs. (13) and (15) and given as respectively 0.140 and 0.939. These calculated values closely matched the sub-optimum design values proposed by Chey, Chase, et al. [30]. In order to compute the damping ratio and frequency of the structure, they are governed by Eqs. (16) and (17).

$$\omega_n = \sqrt{\frac{k}{m}} \quad (16)$$

$$\xi = \frac{c}{2\sqrt{km}} \quad (17)$$

Then, the stiffness and damping of the TMD are computed by governing equations provided below.

$$k_d = m_d\omega_d^2 \quad (18)$$

$$c_d = 2\xi_d\sqrt{k_d m_d} \quad (19)$$

4.4. Optimal control for actively controlled structure

In addition to TMD, ATMD can adapt itself during dynamic loading. Although ATMD is a so promising control strategy, it has some significant disadvantages such as time delays, output measurement errors, phase lag effects especially in the verification of experimental study. In the present work, such disadvantages and their effects on structural performance are ignored for simplification in the simulation of seismic analysis.

In the control problem, the main purpose is to find control $U(t)$ that minimizes a cost function (J) subject to the constraints of the plant dynamics. General cost function (J) is given by

$$J = \int_0^\infty [Z(t)^T Q Z(t) + U(t)^T R U(t)] dt \quad (20)$$

$$Q = N^T N \in \mathbb{R}^{2n \times 2n} \quad (21)$$

$$R \in \mathbb{R}^{m \times m} \quad (22)$$

where Q is semi-positive definite and R positive definite matrices. If (A, B) is stabilizable and (A, N) is detectable, the solution of the optimal control problem exists and is unique. Where $K \in \mathbb{R}^{2n \times 2n}$ and is semi positive definite, the solution of the Control Algebraic Riccati Equation (CARE) is given in Eq. (20). Matlab is employed in order to get the CARE solution.

$$KA + A^T K + Q - KBR^{-1}B^T K = 0 \quad (23)$$

The matrices (Q and R) are a respectively state-weighting matrix and control-weighting matrix, indicating the relative importance between the control forces and the structural response quantities. If Q matrix is assigned to large values, this gives priority to response reduction over the control force required. Also, If R is defined with large values, it shows great importance to the control force that the actuator provides. Therefore, Q and R matrices are defined according to the relationship between control energy consumption and control effectiveness [32]. In this paper, the first story displacement of the structure ($X_1(t)$) is picked for desired state variable for the maximum reduction, see in Eq. (24). Hence Q and R matrices are defined as below.

$$J = \int_0^\infty [X_1(t)^T Q X_1(t) + U(t)^T R U(t)] dt \quad (24)$$

In which, Q is equal to 12.10^4 and R is 10^{-12} . Excluding the earthquake base excitation, Riccati closed loop control (the control vector) $U(t)$ is given by

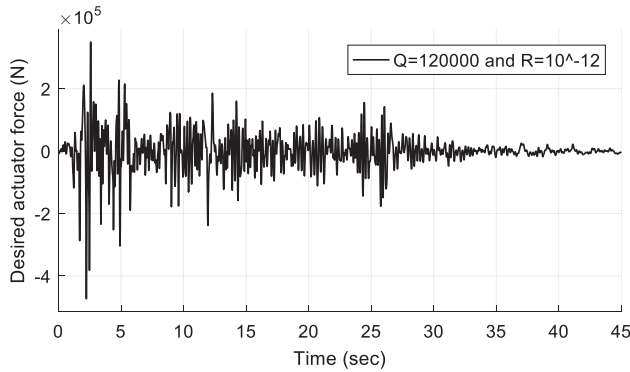


Fig. 6. Desired actuator force (N).

$$U(t) = -GZ(t) \quad (25)$$

$$G = R^{-1}B^TK \quad (26)$$

Substituting Eq. (25) into Eq. (9), the closed loop of the actively controlled structure becomes:

$$\dot{Z}(t) = (A - BG)Z(t) + BU(t) + Wx''_g(t) \quad (27)$$

4.5. Actuator location & actuator dynamics

Many studies so far have used single and multi-actuators implementation either on the first or any number of floors of the structure. Installation of the actuator at every floor, in practice, is extremely expensive and may not be applicable in consideration of dynamic of actuators. There are plenty of electric and mechanical components such as sensors, transducers, and a computer that are cooperated in order to operate the control system. Therefore, the system with fewer actuators may be more realistic in terms of cost and simplicity.

Another important concern about actuators is the maximum force that they can provide. In the case of a strong earthquake, this limitation will be exceeded where the actuator will not be able to deliver the required control force. Therefore, it is essential to design controllers to reduce structural damage and prevent total structural failure in the event of a strong earthquake [33].

In this study, the force (approximately a maximum value of 485 kN) the actuator needs to generate, driven by the LQR controller, is illustrated in Fig. 6 with the selection of Q and R parameter. MTS 244 or 243 series actuator for civil structures might be employed to perform the dynamic scenario. For more detailed information, the readers are referred to [34].

5. Simulation results and discussion

A 6-story of RC building were modeled, and the analyses are respectively conducted on the RC building by retrofitting with the placement of the infill walls layout, the implementation of TMD and ATMD, see Fig. 4.

In order to illustrate the effect of the infill wall in the dynamic analysis, the results are obtained and compared with the RC building and the RC building with TMD and ATMD. As seen in Table 5, the infill wall significantly increases the frequencies of the structure, which is vital for the effectiveness of TMD and ATMD in the tuning process. It has also a substantial amount of stiffness contribution (lateral bearing load capacity) and damping contribution (energy dissipation capacity), see Table 4.

After tuning TMD and ATMD to the fundamental frequency (16.7 rad/sec) of the RC building and its dynamic properties are provided in Table 4, the maximum response of the structures at the resonance frequency and their phase angle are obtained and compared one another, see in Fig. 7.

As seen in Fig. 7, RC building gives the highest peak amplitude at the fundamental natural circular frequency. It is observed that TMD and ATMD highly suppress the magnitude of the response at the resonant frequency. However, the infill wall makes the amplitude suppressed and forwarded to the higher frequency thanks to the significant amount of stiffness contribution to the system. Because of the fact that it changes the natural frequency, its phase response is step-forwarded as compared to the rest. As well as, the RC building and TMD/ATMD gives the different magnitudes at the same frequency, however, it reached the peak response at the different frequency. This is because TMD and ATMD are tuned to the first natural frequency.

The time history simulations are performed in Matlab/Simulink and it is observed from the results that the RC building experiences the highest peak amplitude (7.83 mm) in the first floor, see Fig. 8. When it is respectively retrofitted with the infill wall, TMD and ATMD, there is a reduction in the peak response of 68%, 17% and 32% on the first floor. Similarly, the reductions in the roof floor are respectively 69%, 15% and 34% as compared to the bare RC building. There are also significant reductions in the peak acceleration both the first and the roof floor, see Table 6.

The root mean square (RMS) is an important parameter, which is used to measure the intensity of vibration, to evaluate accumulative structural response and energy. Table 6 also shows the comparison of the RMS results of displacement and acceleration for each of the structures. A reduction of 71%, 24% and 52% in the first-floor absolute acceleration is obtained under El Centro excitation. For the roof floor, the reductions are respectively founded 70%, 18% and 50% which are slightly different comparing the first-floor reduction except the RC building with ATMD.

The inter-story drift is another useful response quantity for structural (earthquake) engineers, especially for high-rise buildings. Inter-story drifts can be reduced in the first floor from 0.26% to 0.08%, 0.22% and 0.17% by strengthening the RC building respectively with infill wall, TMD and ATMD for El Centro earthquake. It is important to note that the infill wall was superior to the TMD and ATMD in terms of inter-story drift performance (see Fig. 9).

The input energy (E_{ir}) to a structure is introduced as a new measure of criticality during an earthquake and it depends proportional to the relationship between relative velocity and the ground acceleration [35]. The RC building actively controlled by ATMD has the maximum energy with 393 kN m as well as its

Table 5
The first five modal frequencies of the structures.

Modal frequency (Hz)	RC building	RC building with infill wall	RC building with TMD	RC building with ATMD
Mod. 1	2.67	4.54	2.22	2.22
Mod. 2	7.85	13.35	2.99	2.99
Mod. 3	12.58	21.39	7.89	7.89
Mod. 4	16.57	28.19	12.59	12.59
Mod. 5	19.60	33.34	16.58	16.58

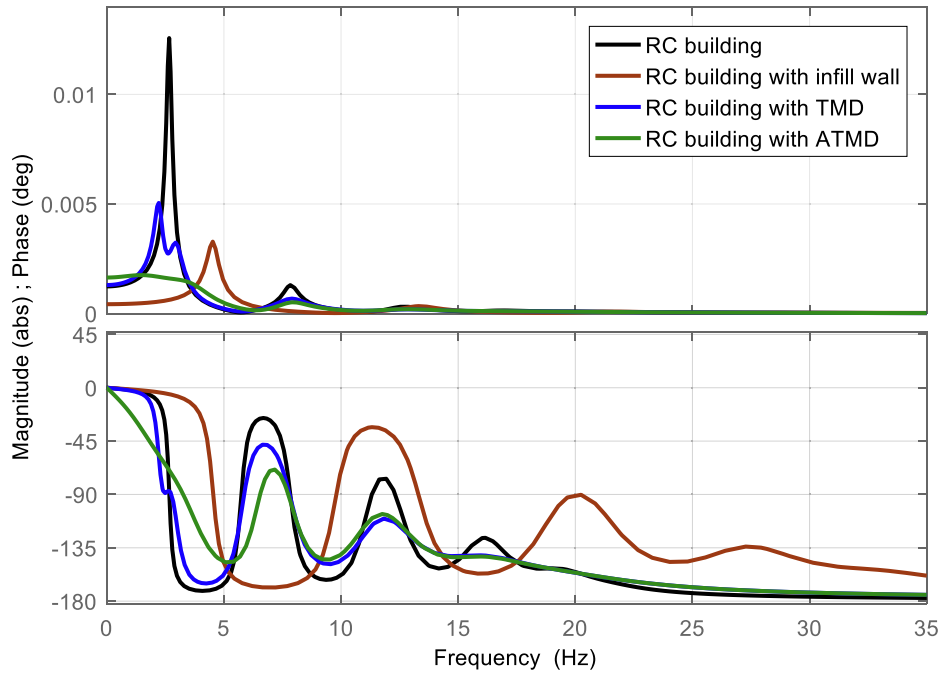


Fig. 7. Bode diagram for the first floor of the structures.

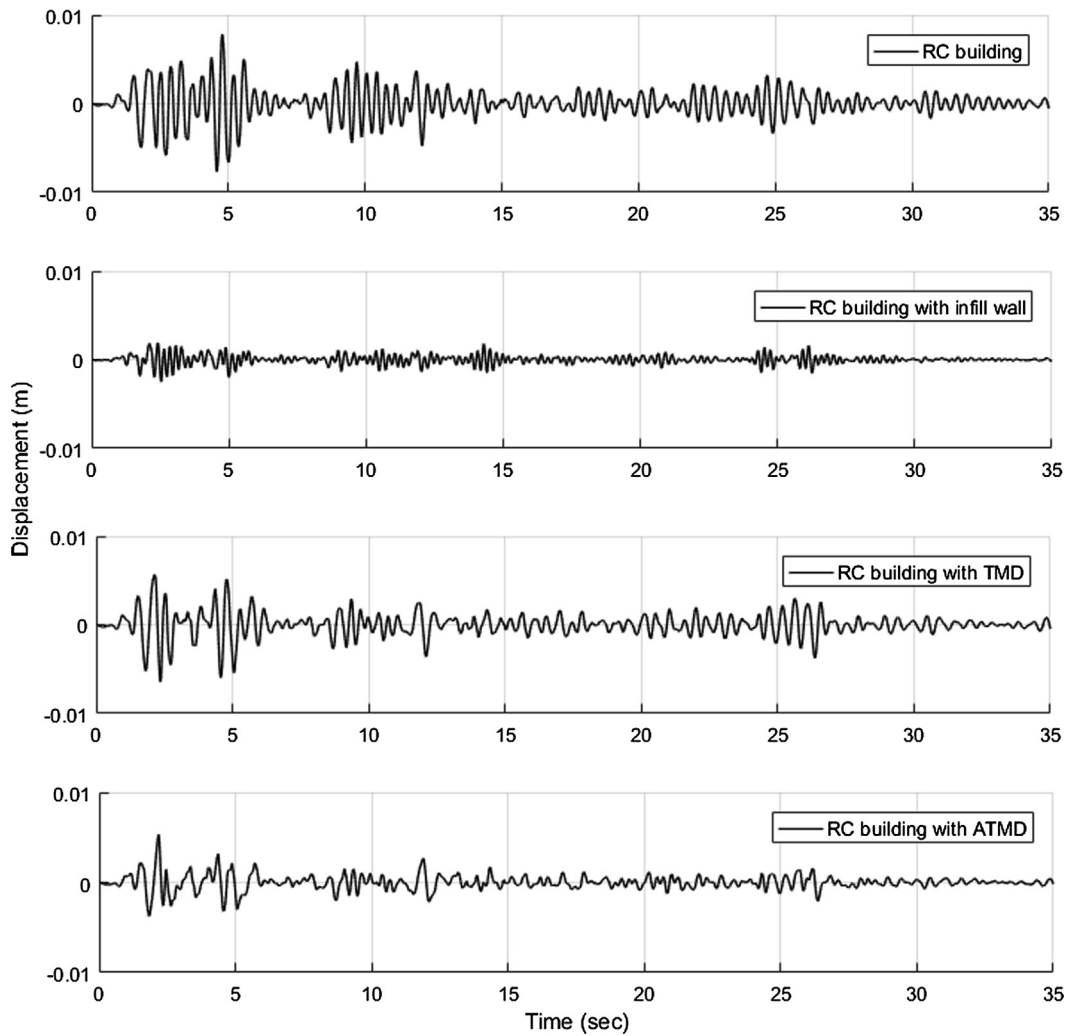


Fig. 8. The first-floor relative displacements of the structures.

Table 6
The response of the structures.

Type of structures	Displacements				Accelerations			
	The first floor		The top floor		The first floor		The top floor	
	Peak (mm)	RMS (mm)	Peak (mm)	RMS (mm)	Peak (mm/s ²)	RMS (mm/s ²)	Peak (mm/s ²)	RMS (mm/s ²)
RC building	7.83	1.5	32.88	5.9	2640	435.8	9260	1641
RC building with infill wall	2.47	0.43	10.06	1.74	2150	314.3	7800	1284
RC building with TMD	6.47	1.14	27.79	4.81	2417	285.4	8167	1122
RC building with ATMD	5.29	0.72	21.11	2.91	2636	222.1	5933	728

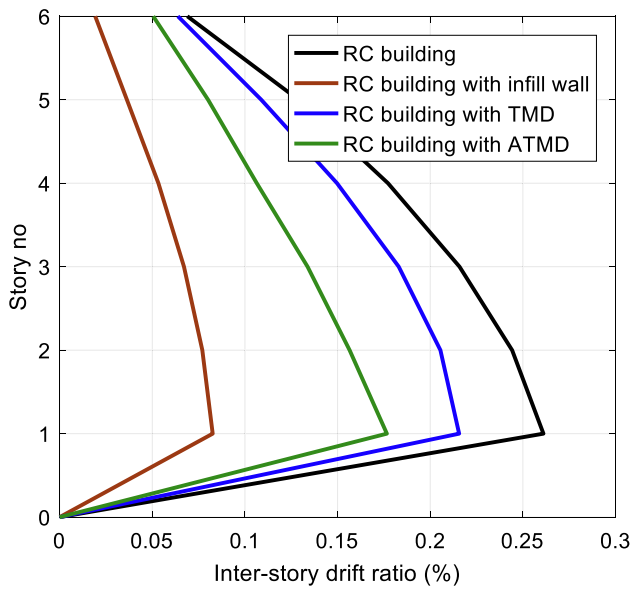


Fig. 9. Maximum inter-story drift ratio of the structures.

maximum kinetic energy is the maximum with 34.5 kN m, because it has the fastest relative velocity among the others. The RC building with infill wall has the minimum input energy among the others, which means that it is subjected to less dynamic energy under earthquake loadings. Furthermore, the structure, controlled by TMD is with the earthquake input energy (191 kN m), which is less than the one with ATMD. Thus, in this circumstance, ground accelerations and actuator energy are playing an important role in the input energy of the structures, see Table 7.

The strain energy is another indicator to test structural performance and it has a strong relationship to the structural damages. The bearing systems of a structure; columns and beams have capacities that can dissipate energy safely. If those capacities are exceeded, structural damages could be the outcome under earthquakes. In a comparison of the strain energy between the models, the bare RC building has the highest strain energy of $E_a = 69$ kN m. The RC building with infill wall has the lowest strain energy of $E_a = 41.9$ kN m, followed by the building model with TMD with $E_a = 51.2$ kN m and building model with ATMD with $E_a = 55.8$ kN m. This is because strengthening the RC building by the infill wall significantly improves the lateral load capacity, so it maximizes the response reduction among others. Fig. 10 illustrates the total energy graphs for various building type.

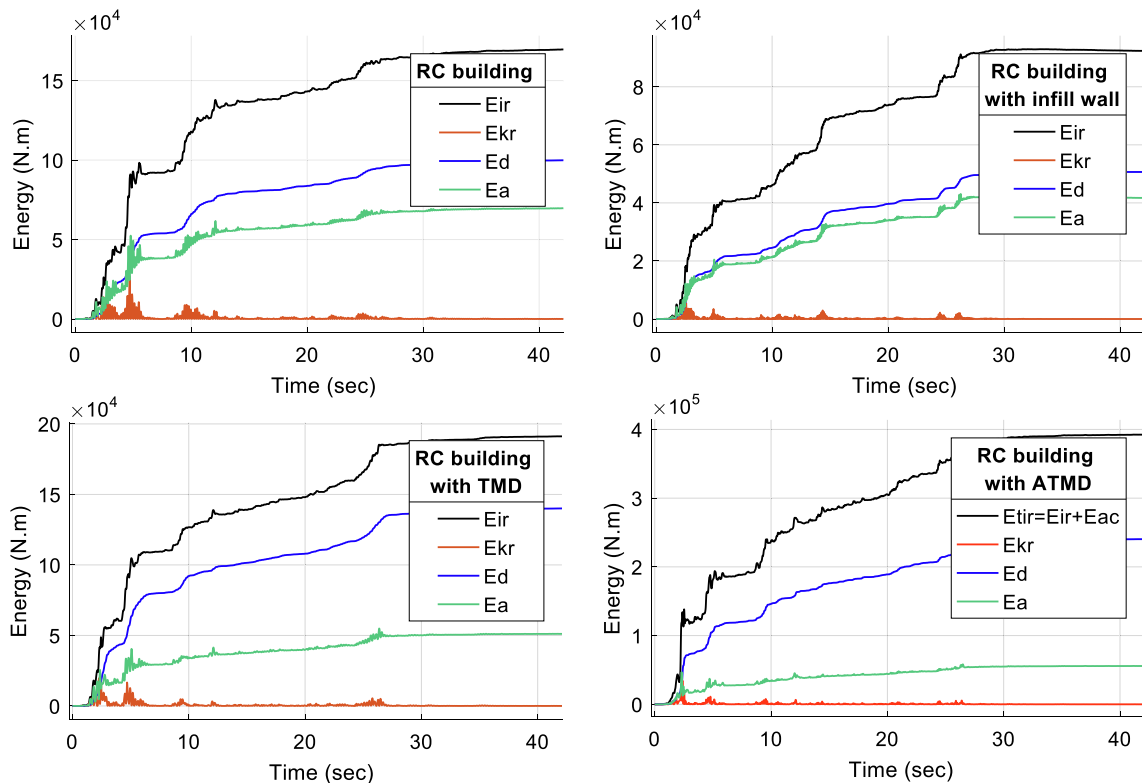


Fig. 10. Total energy graphs for the model structures.

Table 7
The total energy of the structures.

Type of structures	The total energy				
	Peak kinetic energy (E_{kr}) (kN m)	Damping energy (E_d) (kN m)	Strain energy (E_a) (kN m)	Input energy (E_{ir}) (kN m)	Actuator energy (E_{ac}) (kN m)
RC building	27.1	100	69	169	N/A
RC building with infill wall	5.4	50.5	41.9	92.4	N/A
RC building with TMD	19.7	140	51.2	191	N/A
RC building with ATMD	34.5	241.2	55.8	393	96

Unlike TMD and ATMD, the structure with infill wall has the lowest damping energy (50.5 kN) even though there is a 33% increase in the damping ratio as compared to the bare structure. This is due to the fact that the velocity response is significantly decreased by the inclusion of the infill wall. Implementing, in ascending order, of the TMD and ATMD on the bare RC building, increases from 140 to 241.2 kN m in the damping energy. The active and passive controllers dissipate the dynamic energy by taking advantages of the phase difference between the controller mass and the main structure, on the other hand, the infill wall can reduce the undesirable energy by increasing lateral load and damping capacity, in addition, the bare structure.

In short, it is obvious that the structure with infill wall overall performs the best among others, however, the performance of the structure with TMD and ATMD can be upgraded by adding multiple TMDs either at the first or any floors and the actuators on the bare system to increase the effectiveness and to suppress undesirable response and energy, see Table 7.

6. Conclusions

The purpose of this paper was to examine and investigate the effect of the masonry infill wall, which is generally neglected when the structure is subjected to dynamic loading. Additionally, the RC building is passively (TMD) and actively (ATMD) controlled for comparison purposes and for verifying the effectiveness of the infill wall. The following conclusions were pointed out from the numerical results:

1. The infill wall has a significant effect on the fundamental frequency of the structure, which is also vital in tuning process of TMD and ATMD, especially in case the structure with infill wall layout wants to be controlled actively and passively. As well as, infill wall increases significantly the rigidity (190% increase) and the damping (150% increase) of the structures when it is fully symmetrically placed into the frame and it performs as a structural element during an earthquake.
2. The strain energy (E_a) has a strong relationship to the damage level of the structural components. Thus, the infill wall, which has the lowest the strain energy, could be the securest energy dissipater system in terms of energy instead of using TMD and ATMD.
3. The infill wall is very effective to restrict inter-story drift ratio as compared to the others because its damping and stiffness contribution to the bare RC building is very sufficient.
4. In the RMS and peak displacement/acceleration for the first and roof floor, the effectiveness of the infill wall is superior to the rest. Therefore, the infill wall can be used for structural control thanks to mostly be used in real life, simple to construct, its cost and its performance without external energy, and mechanical components as compared to TMD and ATMD controller.
5. The performance of the active control device (ATMD) would be improved however its performance depends mostly upon the amount of external source of energy, which is driven by a control methodology such as LQR and LQG.

Acknowledgement

The authors would like to thankfully acknowledge the Ministry of National Education of the Republic of Turkey for providing the opportunity and scholarship during the first author's doctoral study in the United States of America. This research did not receive any specific grant from funding agencies in the public, commercial, or not-for-profit sectors.

References

- [1] Nishimura I, Yamada T, Sakamoto M, Kobori T. Control performance of active-passive composite tuned mass damper. *Smart Mater Struct* 1998;7:637–53. <https://doi.org/10.1088/0964-1726/7/5/008>.
- [2] Arfiadi Y. *Optimal passive and active control mechanisms for seismically excited buildings*. University Of Wollongong; 2000.
- [3] Azimi M, Rasoulnia A, Lin Z, Pan H. Improved semi-active control algorithm for hydraulic damper-based braced buildings. *Struct Control Heal Monit* 2017;24. <https://doi.org/10.1002/stc.1991>.
- [4] De Domenico D, Ricciardi G. An enhanced base isolation system equipped with optimal tuned mass damper inerter (TMDI). *Earthq Eng Struct Dyn* 2018;47:1169–92. <https://doi.org/10.1002/eqe.3011>.
- [5] Hashemi A, Mosalam KM. *Seismic evaluation of reinforced concrete buildings including effects of masonry infill walls*, 2007.
- [6] Akyürek O. *Betonarme Bina Performansına Dolgu Duvarların Etkisi (The effects of infill walls in RC building performance)*. Suleyman Demirel University; 2014.
- [7] Pujol S, Fick D. The test of a full-scale three-story RC structure with masonry infill walls. *Eng Struct* 2010;32:3112–21. <https://doi.org/10.1016/j.engstruct.2010.05.030>.
- [8] Tekeli H, Aydın A. An experimental study on the seismic behavior of infilled RC frames with opening. *Sci Iran* 2017;24:2271–82. <https://doi.org/10.24200/sci.2017.4150>.
- [9] Koçak A, Yıldırım MK. Effects of infill wall ratio on the period of reinforced concrete framed buildings. *Adv Struct Eng* 2011;14:731–43. <https://doi.org/10.1260/1369-4332.14.5.731>.
- [10] Akyürek O, Tekeli H, Demir F. Plandaki Dolgu Duvar Yerleşiminin Bina Performansı Üzerindeki Etkisi (The Effects of Infill Walls Located in Plan on Buildings Performance). *Int J Eng Res Dev* 2018;30:42–55. <https://doi.org/10.29137/umagd.419660>.
- [11] Folhento PLP, Braz-César MT, Paula AM V, Barros RC. Influence of stiffness and strength degradation of an infill wall upon the performance of a TMD; 2018. p. 22–6.
- [12] Das S, Choudhury S, Dey AK. Performance of low-rise RC buildings with tuned liquid dampers (TLDs) in presence of masonry infill. *Asian J Civ Eng* 2017;18:535–46.
- [13] Hartog JP DEN. *Mechanical vibrations*; 1985.
- [14] Villaverde R. *Seismic control of structures with damped resonant appendages*. Proc, First World Conf Struct Control 1994:113–9.
- [15] Li C. Performance of multiple tuned mass dampers for attenuating undesirable oscillations of structures under the ground acceleration. *Earthq Eng Struct Dyn* 2000;29:1405–21. [https://doi.org/10.1002/1096-9845\(200009\)29:9<1405::AID-EQE976>3.0.CO;2-4](https://doi.org/10.1002/1096-9845(200009)29:9<1405::AID-EQE976>3.0.CO;2-4).
- [16] Nigdeli SM, Boduroğlu MH. Active tendon control of torsionally irregular structures under near-fault ground motion excitation. *Comput Civ Infrastruct Eng* 2013;28:718–36. <https://doi.org/10.1111/micc.12046>.
- [17] Jiang BJB, Wei XWX, Guo YGY. Linear quadratic optimal control in active control of structural vibration systems. *Control Decis Conf (CCDC)*, 2010 Chinese 2010:3546–51. <https://doi.org/10.1109/CCDC.2010.5498552>.
- [18] Yanik A, Aldemir U, Bakioglu M. A new active control performance index for vibration control of three-dimensional structures. *Eng Struct* 2014;62:63:53–64. <https://doi.org/10.1016/j.engstruct.2014.01.009>.
- [19] Soong TT. State-of-the-art review. Active structural control in civil engineering. *Eng Struct* 1988;10:74–84. [https://doi.org/10.1016/0141-0296\(88\)90033-8](https://doi.org/10.1016/0141-0296(88)90033-8).
- [20] Kim Y, You K, You J, Paek S, Nam B. LQR control of along-wind responses of a tall building using active tuned mass damper. *2016 World Congr Adv Civ, Environ Mater Res* 2016;2013(421):767–71. <https://doi.org/10.4028/www.scientific.net/AMM.421.767>.

- [21] Akyürek O. Lateral and torsional seismic vibration control for torsionally irregular buildings. Florida Institute of Technology; 2019.
- [22] Shafieezadeh A. DigitalCommons@USU application of structural control for civil engineering structures. Utah State University; 2008.
- [23] Guclu R, Yazici H. Vibration control of a structure with ATMD against earthquake using fuzzy logic controllers. *J Sound Vib* 2008;318:36–49. <https://doi.org/10.1016/j.jsv.2008.03.058>.
- [24] Guclu R, Yazici H. Seismic-vibration mitigation of a nonlinear structural system with an ATMD through a fuzzy PID controller. *Nonlinear Dyn* 2009;58:553–64. <https://doi.org/10.1007/s11071-009-9500-5>.
- [25] MathWorks MATLAB. SIMULINK for technical computing; 2016. Available on <<https://www.mathworks.com>>.
- [26] Federal Emergency Management Agency (FEMA). FEMA 355F – State of the art report on performance prediction and evaluation of steel moment-frame buildings. Fema-355F 2000;1:1–367.
- [27] Clough RW, Penzien J. Dynamics of structures 1995;78. <https://doi.org/10.1103/PhysRevC.78.014905>.
- [28] Dolšek M, Fajfar P. The effect of masonry infills on the seismic response of a four storey reinforced concrete frame—a probabilistic assessment. *Eng Struct* 2008;30:3186–92. <https://doi.org/10.1016/j.engstruct.2008.04.031>.
- [29] Wong KKF, Yang R. Earthquake response and energy evaluation of inelastic structures. *J Eng Mech* 2002;128:308–17. [https://doi.org/10.1061/\(ASCE\)0733-9399\(2002\)128:3\(308\)](https://doi.org/10.1061/(ASCE)0733-9399(2002)128:3(308)).
- [30] Chey Min-Ho, Chase J Geoffrey, Mander John B, CAM. Semi-active tuned mass damper building systems: design. *Earthq Eng Struct Dyn* 2009;39:119–39. <https://doi.org/10.1002/eqe>.
- [31] Abubakar IM, Farid BJM. Seismic control systems: design and performance assessment, vol. 2012. Bostan: WITPRES; 2012.
- [32] Kumar A, Poonama B, Sehgal V. Active vibration control of structures against earthquakes using modern control theory. *ASIAN J Civ* 2007;3:283–99.
- [33] Aaron Samuel Brown. Multi-objective civil structural control incorporating neural networks. Santa Barbara: University of California; 2000. doi:UMI Number 3013206.
- [34] Civil, structural and architectural engineering testing capabilities 4/11 7AD. <http://www.mts.com/cs/groups/public/documents/library/dev_002186.pdf> [accessed September 12, 2018].
- [35] Takewaki I. Bound of earthquake input energy. *J Struct Eng* 2004;130:1289–97. [https://doi.org/10.1061/\(ASCE\)0733-9445\(2004\)130:9\(1289\)](https://doi.org/10.1061/(ASCE)0733-9445(2004)130:9(1289)).